



**HAL**  
open science

## **A-T Volume Integral Formulations for Solving Electromagnetic Problems in the Frequency Domain**

G rard Meunier, Olivier Chadebec, Jean-Michel Guichon, Vinh Le-Van,  
Jonathan Siau, Bertrand Bannwarth, Frederic Sirois

► **To cite this version:**

G rard Meunier, Olivier Chadebec, Jean-Michel Guichon, Vinh Le-Van, Jonathan Siau, et al.. A-T  
Volume Integral Formulations for Solving Electromagnetic Problems in the Frequency Domain. IEEE  
Transactions on Magnetics, 2016, 52 (3), 10.1109/TMAG.2015.2496243 . hal-02277766

**HAL Id: hal-02277766**

**<https://hal.science/hal-02277766v1>**

Submitted on 23 Nov 2020

**HAL** is a multi-disciplinary open access archive for the deposit and dissemination of scientific research documents, whether they are published or not. The documents may come from teaching and research institutions in France or abroad, or from public or private research centers.

L'archive ouverte pluridisciplinaire **HAL**, est destin e au d p t et   la diffusion de documents scientifiques de niveau recherche, publi s ou non,  manant des  tablissements d'enseignement et de recherche fran ais ou  trangers, des laboratoires publics ou priv s.

# A–T Volume Integral Formulations for Solving Electromagnetic Problems in the Frequency Domain

G erard Meunier<sup>1,2</sup>, Olivier Chadebec<sup>1,2</sup>, Jean-Michel Guichon<sup>1,2</sup>, Vinh Le-Van<sup>1,2</sup>,  
Jonathan Siau<sup>1,2</sup>, Bertrand Bannwarth<sup>1,2</sup>, and Fr ed eric Sirois<sup>3</sup>

<sup>1</sup>Grenoble Electrical Engineering Laboratory, Universit  Grenoble Alpes, Grenoble F-38000, France

<sup>2</sup>Grenoble Electrical Engineering Laboratory, Centre National de Recherche Scientifique, Grenoble F-38000, France

<sup>3</sup> cole Polytechnique de Montr al, Montreal, QC H3C 3A7, Canada

**A volume integral formulation for solving electromagnetic problems in the frequency domain is proposed. First, it is based on a magnetic flux and current density face element interpolation for representing the electromagnetic problem through an equivalent circuit. Second, magnetic vector potentials  $A$  and electric vector potential  $T$  are considered, thanks to the use of finite element mesh connectivity matrices. The formulation is particularly well adapted to solving electromagnetic problems with large air domains, in the presence of thin electric regions and magnetic materials.**

*Index Terms*— Electromagnetism, equivalent circuit, face and edge elements, vector potential, volume integral formulation.

## I. INTRODUCTION

**D**IFFERENT works have shown the interest of using volume integral method (VIM) for 3-D magnetic field analysis [15], the main advantage being that the air region does not need to be meshed. In particular, the VIM Partial Element Equivalent Circuit Method has shown great ability to handle really complex devices in the presence of conductors and complex electrical circuits [10], such as power electronic devices, which is the type of problem we want to address. Moreover, in recent years, there was a regain of interest for solving Maxwell’s equations by Green’s function integrals triggered by the development of matrix compression algorithms, which greatly improves storage and resolution of full matrix systems.

On the other hand, Whitney face interpolation for current density  $\mathbf{J}$  and magnetic flux density  $\mathbf{B}$  is well suited for representing an electromagnetic problem through an equivalent circuit [2]. This approach provides a solution that ensures the conservation of flux and current through the facets of the mesh [3]. In this work, we propose an alternative vector potential approach derived from the previous method.

## II. EQUIVALENT CIRCUIT APPROACH THROUGH FACET ELEMENT AND VOLUME INTEGRAL FORMULATION

Let us consider a linear magnetodynamic problem with magnetic regions  $\Omega_m$  (presence of magnetization  $\mathbf{M}$ ), conducting electrical regions  $\Omega_c$  (presence of current density  $\mathbf{J}$ ), and coils (imposed current density  $\mathbf{J}_0$ ). The two constitutive laws linking the current density  $\mathbf{J}$  to the electric field  $\mathbf{E}$  (in  $\Omega_c$ ) and the flux density  $\mathbf{B}$  to the magnetic field  $\mathbf{H}$  (in  $\Omega_m$ ) are expressed as follows:

$$\mathbf{J} = \sigma \mathbf{E} \quad \mathbf{M} = \chi \mathbf{H} = (\nu_0 - \nu) \mathbf{B}. \quad (1)$$

We can express the electric field  $\mathbf{E}$  and the magnetic field  $\mathbf{H}$  through vector potentials (magnetic  $\mathbf{A}$  and electric  $\mathbf{T}$ ) and scalar potentials (electric  $V$  and magnetic  $\phi$ ) such as

$$\begin{aligned} \mathbf{E} &= -j\omega \mathbf{A} - \mathbf{grad} V & \mathbf{H} &= \mathbf{T} - \mathbf{grad} \phi \\ \mathbf{A}(P) &= \frac{\mu_0}{4\pi} \left( \int_{\Omega_c} \frac{\mathbf{J}(Q)}{r} d\Omega + \int_{\Omega_0} \frac{\mathbf{J}_0(Q)}{r} d\Omega \right. \\ &\quad \left. + \int_{\Omega_m} \frac{\mathbf{M}(Q) \wedge \mathbf{r}}{r^3} d\Omega \right) \\ \mathbf{T}(P) &= \frac{1}{4\pi} \int_{\Omega_c} \frac{\mathbf{J}(Q) \wedge \mathbf{r}}{r^3} d\Omega & \phi(P) &= \frac{1}{4\pi} \int_{\Omega_m} \frac{\mathbf{M}(Q) \cdot \mathbf{r}}{r^3} d\Omega \end{aligned} \quad (2)$$

where  $\omega$  is the angular frequency and  $r$  is the distance between point  $P$  and integration point  $Q$  in  $\Omega_c$  and  $\Omega_m$ . Meunier *et al.* [3] proposed to solve electromagnetic problems through a volume integral formulation based on the first-order face elements discretization for  $\mathbf{B}$  and  $\mathbf{J}$  (the mesh is limited to  $\Omega_m$  for  $\mathbf{B}$  and to  $\Omega_c$  for  $\mathbf{J}$ )

$$\mathbf{J} = \sum_j \mathbf{w}_j I_j \quad \mathbf{B} = \sum_g \mathbf{w}_g \Psi_g \quad (3)$$

where  $\mathbf{w}_j$  and  $\mathbf{w}_g$  are the face shape functions, and  $I_j$  and  $\Psi_g$  the electric and magnetic fluxes, respectively. In practice, integral volume formulation consists in matching electric and magnetic fields obtained by (1) with electric and magnetic fields expressed by local laws (2). It can be achieved by applying two Galerkin procedures, respectively, associated with  $\Omega_c$  and  $\Omega_m$  and by using previous face shape functions  $\mathbf{w}_j$  and  $\mathbf{w}_g$  for projection

$$\int_{\Omega_c} \mathbf{w}_i \cdot \left( \frac{\mathbf{J}}{\sigma} - \mathbf{E} \right) d\Omega = 0 \quad \int_{\Omega_m} \mathbf{w}_f \cdot \left( \frac{\mathbf{M}}{\chi} - \mathbf{H} \right) d\Omega = 0. \quad (4)$$

Equation (4) allows us to build two equivalent circuits for magnetic (Fig. 1) and electric regions, whose graphs are dual meshes of the primal meshes used for  $\Omega_m$  and  $\Omega_c$ . Inserting (2) and (3) in (4) provides

$$\begin{bmatrix} R + j\omega L & Y \\ X & K + M \end{bmatrix} \begin{Bmatrix} I \\ \Psi \end{Bmatrix} = \begin{Bmatrix} \Delta V \\ \Delta \Phi \end{Bmatrix} + \begin{Bmatrix} U \\ Q \end{Bmatrix}$$

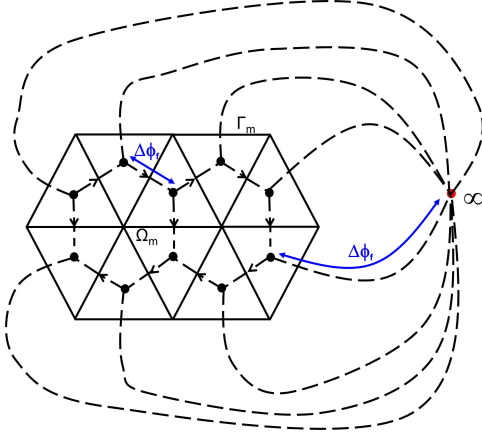


Fig. 1. Circuit representation for magnetic regions.

which allow to express magnetic and electric potential differences  $\{\Delta\Phi\}$  and  $\{\Delta V\}$  on the branches of the equivalent circuits [3]. Matrix coefficients are

$$\begin{aligned}
 R_{ij} &= \int_{\Omega_c} \mathbf{w}_i \cdot \frac{\mathbf{w}_j}{\sigma} d\Omega & L_{ij} &= \frac{\mu_0}{4\pi} \int_{\Omega_c} \mathbf{w}_i \cdot \int_{\Omega_c} \frac{\mathbf{w}_j}{r} d\Omega d\Omega \\
 Y_{ig} &= j\omega \frac{\mu_0}{4\pi} \int_{\Omega_c} \mathbf{w}_i \cdot \int_{\Omega_m} (v_0 - v) \frac{\mathbf{w}_g \wedge \mathbf{r}}{r^3} d\Omega d\Omega \\
 K_{fg} &= \int_{\Omega_m} \mathbf{w}_f v \mathbf{w}_g d\Omega \\
 M_{fg} &= \frac{1}{4\pi} \int_{\Gamma_f} \frac{1}{S_f} \int_{\Omega_m} (v - v_0) \frac{\mathbf{w}_g \cdot \mathbf{r}}{r^3} d\Omega d\Omega \\
 X_{fj} &= -\frac{1}{4\pi} \int_{\Omega_c} \mathbf{w}_f \cdot \int_{\Omega_m} \frac{\mathbf{w}_j \wedge \mathbf{r}}{r^3} d\Omega d\Omega
 \end{aligned} \quad (6)$$

and source terms produced by  $k$  coils are, for example

$$\begin{aligned}
 U_i &= -j\omega \frac{\mu_0}{4\pi} \int_{\Omega_c} \mathbf{w}_i \cdot \sum_k \left( \int_{\Omega_0} \frac{\mathbf{j}_{0k}}{r} d\Omega \right) I_k d\Omega \\
 Q_f &= \frac{1}{4\pi} \int_{\Omega_m} \mathbf{w}_f \cdot \sum_k \left( \int_{\Omega_0} \frac{\mathbf{j}_{0k} \wedge \mathbf{r}}{r^3} d\Omega \right) I_k d\Omega
 \end{aligned} \quad (7)$$

where  $\mathbf{j}_{0k}$  is the source vector current density, which produces a current of 1 A in coil  $k$  and  $I_k$  is the current flowing through coil  $k$ . System (5) can be solved by the use of a circuit solver by using mesh analysis. Circuit equations  $M_m\{\Delta\Phi\} = 0$  and  $M_c\{\Delta V\} = 0$  [3], where  $M_c$  and  $M_m$  are the branch-fundamental independent loop matrices, allow strongly imposing the solenoidality of the magnetic flux  $\mathbf{B}$  and current density  $\mathbf{J}$ . The unknowns are mesh currents and fluxes such as  $\{I\} = M_c\{I_M\}$  and  $\{\Psi\} = M_m\{\Psi_M\}$ . The formulation can be easily extended to the case of thin regions by introducing an equivalent surface representation [12]. In Section III, we propose to solve equations (5) by an alternative vector potentials  $A$ - $T$  formulation.

### III. SIMPLY CONNECTED $A$ - $T$ FORMULATION

Let us consider usual connectivity matrices of primal magnetic and electric finite element meshes:  $G_m$  and  $G_c$  between edges and nodes,  $C_m$  and  $C_c$  between faces and edges, and  $D_m$  and  $D_c$  between volumes and faces. Matrices of the

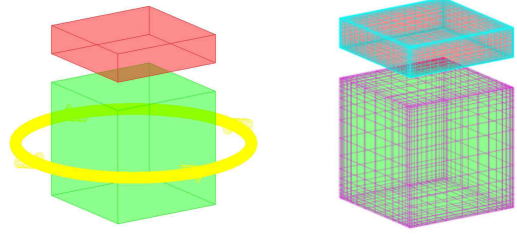


Fig. 2. Geometry and mesh of the test: a magnetic region ( $\mu_r = 100$ ) surrounded by a coil and a conducting region ( $\sigma = 6e + 7$  S/m) above.

dual complex on  $\Omega_m$  are then defined by  $\tilde{G}_m$ ,  $\tilde{C}_m$  and  $\tilde{D}_m$ , with  $\tilde{G}_m = D_m^t$ ,  $\tilde{C}_m = C_m^t$ ,  $\tilde{D}_m = -G_m^t$  [4], [5]. Similar relations are used for  $\tilde{G}_c$ ,  $\tilde{C}_c$ ,  $\tilde{D}_c$  on  $\Omega_c$ .

On the primal meshes, on which  $\mathbf{B}$  and  $\mathbf{J}$  are interpolated, the connectivity matrices  $C_m$  and  $C_c$  link the integrals of magnetic and electric vector potential (denoted  $\mathbf{A}$  and  $\mathbf{T}$ ) along the edges  $e$  of each facet  $f$ , with  $\Psi$  and  $I$  being the magnetic fluxes and the currents through faces

$$\begin{aligned}
 \{\Psi\} &= C_m\{\mathbf{A}\} \left( \Psi_f = \iint_f \mathbf{B} dS = \sum_{\text{edges } e} \int_e \mathbf{A} d\mathbf{l} = \sum_e A_e \right) \\
 \{I\} &= C_c\{\mathbf{T}\} \left( I_f = \iint_f \mathbf{J} dS = \sum_{\text{edges } e} \int_e \mathbf{T} d\mathbf{l} = \sum_e T_e \right).
 \end{aligned} \quad (8)$$

On the dual meshes, which define the equivalent circuits, the connectivity gradient matrices  $\tilde{G}_m$  and  $\tilde{G}_c$  link edges and nodes such as

$$\{\Delta\Phi\} = \tilde{G}_m\{\Phi\} \{\Delta V\} = \tilde{G}_c\{V\}. \quad (9)$$

By considering that  $\tilde{G} = D^t$  and  $D \cdot C = 0$  [4], we have

$$C_m^t\{\Delta\Phi\} = C_m^t D_m^t\{\Phi\} = 0, \quad C_c^t\{\Delta V\} = C_c^t D_c^t\{V\} = 0. \quad (10)$$

By letting (8) and (9) in (5), we obtain a novel dense and non-symmetric system (11) to be solved

$$\begin{bmatrix} C_c^t Z_c C_c & C_c^t Y C_m \\ C_m^t X C_c & C_m^t Z_m C_m \end{bmatrix} \begin{bmatrix} T \\ A \end{bmatrix} = \begin{bmatrix} C_c^t U \\ C_m^t Q \end{bmatrix} \quad (11)$$

with  $Z_c = R + j\omega L$  and  $Z_m = K + M$ .

### IV. NUMERICAL RESULTS

We have tested the  $A$ - $T$  formulation on the problem proposed in [3] (Fig. 2). Integrals of Green's kernels of  $L$ ,  $M$ ,  $X$ , and  $Y$  matrices are computed with the use of analytical integrations [7], [8]. No boundary condition is imposed on  $A$ , and  $T = 0$  is imposed on the boundary of conducting regions. Note that the volume integral matrix of magnetic interactions  $M$  can be transformed to a surface integration when the problem is linear [13]. This is not the case in the presence of volume electric regions, since we have to compute full interaction matrices  $L$ ,  $X$ , and  $Y$ . This can be a limitation of VIM formulation in the presence of strong skin effect. A reference solution is obtained with a  $T - \phi$  finite element method (FEM) from 0 to 1000 Hz. A mesh of 3700 elements is used for the volume integral  $A$ - $T$  formulation, which provides

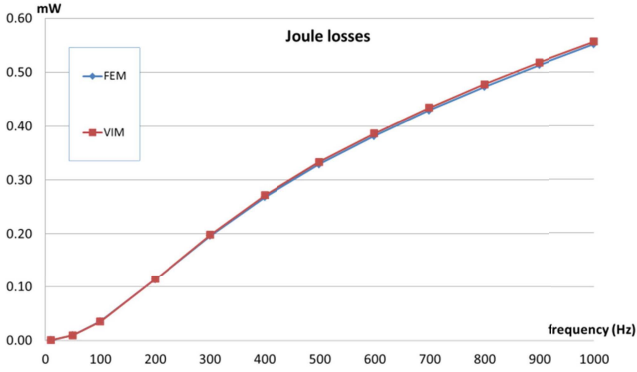


Fig. 3. Comparison of eddy current losses computed by FEM and VIM.

TABLE I  
NUMBER OF GMRES ITERATIONS FOR  $A-T$  AND  $I_M-\Psi_M$   
FORMULATIONS WITH AND WITHOUT USING  
A PRECONDITIONER (100 Hz/1000 Hz)

	Without preconditioner	ILU factorization on FEM matrix	LU factorization on FEM matrix
A-T	113 / 117	29 / 45	26 / 36
$I_M-\Psi_M$	2064 / 2306	86 / 100	83 / 99

a solution close to the FEM one. In Fig. 3 the maximum discrepancy from the FEM is about 1.5% of eddy current losses.

The  $A-T$  formulation has the advantage of not requiring the determination of independent loops. Moreover, since the system of equations is compatible, an iterative solver provides a solution without gauge condition [6], and a better convergence is observed with  $A-T$  formulation in comparison with the  $I_M-\Psi_M$  formulation proposed in [3]. Table I compares the number of iterations when using a Generalized Minimal Residual Method (GMRES) solver, with and without the use of preconditioners. Two preconditioners have been used: complete Lower Upper (LU) factorization (with shift) and incomplete LU factorization (ILU) on the finite element matrices  $R$  and  $K$ .

We note that the use of  $A-T$  formulation provides a good convergence without the use of a gauge even without preconditioning. On the other hand, the use of LU or ILU factorization on the FEM matrices allows obtaining an important reduction of the number of iterations in both cases. In practice,  $I_M-\Psi_M$  and  $A-T$  formulations use the same type of unknowns, e.g., mesh fluxes and mesh currents, acting on the same circuit, i.e., the dual finite element mesh. Indeed,  $\mathbf{T}$  and  $\mathbf{A}$  unknowns represent mesh currents and fluxes around each edge such as  $\{I\} = C_c\{T\}$  and  $\{\Psi\} = C_m\{A\}$ . We can observe that in the general case,  $C_c$  and  $C_m$  provide a set of non-independent loops, unlike the case of matrices  $M_c$  and  $M_m$ . In both cases, the divergence free of flux and current density is strongly imposed.

## V. EXTENSION TO NON-SIMPLY CONNECTED PROBLEMS

Based on circuit representation and mesh analysis, the formulation  $I_M-\Psi_M$  proposed in [3] allows connecting any

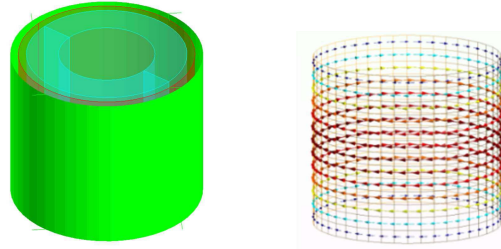


Fig. 4. Test geometry and current density on the conducting region.

external electrical circuit and avoiding any connectivity problem.

On the other hand, in presence of non-simply connected electrical problems, the use of matrix  $C_c$  for  $A-T$  formulation no longer holds, since the necessary loops around the holes are not taken into account [9], [11]. A simple solution consists in substituting the connectivity matrix  $C_c$  by a fundamental branch independent loop matrix  $M_c$ , which can be given by a circuit solver [14]. System (11) becomes

$$\begin{bmatrix} M_c^t Z_c M_c & M_c^t Y C_m \\ C_m^t X M_c & C_m^t Z_m C_m \end{bmatrix} \begin{Bmatrix} I_M \\ A \end{Bmatrix} = \begin{Bmatrix} M_c^t U \\ C_m^t Q \end{Bmatrix}. \quad (12)$$

This formulation is then general and allows solving any type of magnetodynamic problem in the presence of magnetic and electric volume regions, including external circuits.

In order to efficiently get  $M_c$ , we propose a specific algorithm, which combines the use of connectivity matrix  $C_c$  and independent loops search. The  $C_c$  matrix is first easily obtained from the finite element mesh. Then, a specific algorithm dedicated to circuit solver [14] analyzes this matrix on the dual finite element mesh circuit. In the presence of non-simply connected regions, the incidence matrix  $C_c$  is then completed to consider missing loops.

With thin regions, i.e., using a surface mesh, the initial  $C_c$  matrix leads directly to an independent branch loop matrix in the case of simply connected regions. For a non-simply connected region, the number of supplementary loops is then determined by circuit analysis. For instance, in the case of a torus, two supplementary loops are found corresponding to the eddy currents, which can circulate along the torus and the section. In the 3-D volume regions, the  $C_c$  matrix represents a branch loop matrix that is not independent in the general case. The circuit analysis allows eliminating superfluous loops (if desired) and adding the loops due to the presence of holes.

We tested our formulation on a strong magnetic-electric coupling problem. In order to validate on a reliable reference solution, we solved in 3-D an axisymmetric problem composed of a volume magnetic region (average radius 4 mm, thickness 2 mm, height 10 mm, relative permeability = 100), a thin surface copper region (radius 5.5 mm, thickness 0.1 mm, height 10 mm, conductivity  $55 \times 10^6$  S/m), surrounded by a thin surface coil (radius 6 mm, thickness 0.1 mm, height 10 mm) (Fig. 4). The reference solution is an axisymmetric finite element solution associated with a very fine mesh. The 3-D mesh of the VIM method is composed of 572 quadrangles for the conducting region and 1728 tetrahedras for the magnetic region.

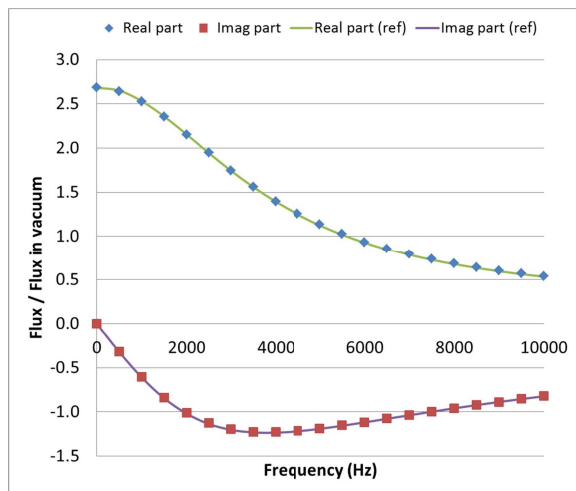


Fig. 5. Comparison of the flux in the coil (real part and imaginary part) obtained by FEM (ref) and VIM.

The  $M_c$  matrix is obtained by the completion of the  $C_c$  matrix, with one supplementary loop found through circuit analysis, and all the initial loops being preserved. In order to compare our solution with the axisymmetric finite element reference one, we compute the flux linkage of the coil for various frequencies between 0 and 10 kHz. The magnetic flux  $\phi$  in a coil  $k$  is given by

$$\phi_k = \int_{\Omega_{0k}} \mathbf{j}_{0k} \cdot \mathbf{A} d\Omega_0. \quad (13)$$

Fig. 5 shows the variation of the flux in the coil versus the frequency. At 0 Hz, in the presence of the magnetic region, the flux in the coil is about 2.7 times higher than the flux obtained in vacuum. When the frequency increases, eddy currents act as a shield and the flux decreases. We note the very good agreement obtained between the two simulations (difference lower than 0.4% at any frequency). The number of iterations with GMRES is 103 against 156 with the use of the formulation  $I_M-\Psi_M$ .

## VI. CONCLUSION

The volume integral approach combining  $\mathbf{A}$  for magnetic region and  $\mathbf{T}$  for electric regions is particularly well suited to model electromagnetic devices with a large air domain. The formulation allows taking into account both magnetic and simply or non-simply connected conducting region.

The formulation is based on circuit representation, where integrations are realized with the use of face interpolation. Particular attention is paid to accurately integrating the Green kernel for closed interactions. The final system of equations can be solved with an iterative solver without imposing a gauge condition.

## REFERENCES

- [1] P. Alotto, F. Desideri, F. Freschi, A. Maschio, and M. Repetto, "Dual-PEEC modeling of a two-port TEM cell for VHF applications," *IEEE Trans. Magn.*, vol. 47, no. 5, pp. 1486–1489, May 2011.
- [2] A. Demenko and J. K. Sykulski, "Geometric formulation of edge and nodal finite element equations in electromagnetics," *COMPEL-Int. J. Comput. Math. Elect. Electron. Eng.*, vol. 31, no. 5, pp. 1347–1357, 2012.
- [3] G. Meunier, O. Chadebec, and J.-M. Guichon, "A magnetic flux–electric current volume integral formulation based on facet elements for solving electromagnetic problems," *IEEE Trans. Magn.*, vol. 51, no. 3, Mar. 2015, Art. ID 7001704.
- [4] A. Bossavit and L. Kettunen, "Yee-like schemes on staggered cellular grids: A synthesis between FIT and FEM approaches," *IEEE Trans. Magn.*, vol. 36, no. 4, pp. 861–867, Jul. 2000.
- [5] R. Specogna and F. Trevisan, "Eddy-currents computation with T- $\Omega$  discrete geometric formulation for an NDE problem," *IEEE Trans. Magn.*, vol. 44, no. 6, pp. 698–701, Jun. 2008.
- [6] Z. Ren, "Influence of the RHS on the convergence behaviour of the curl-curl equation," *IEEE Trans. Magn.*, vol. 32, no. 3, pp. 655–658, May 1996.
- [7] M. Fabbri, "Magnetic flux density and vector potential of uniform polyhedral sources," *IEEE Trans. Magn.*, vol. 44, no. 1, pp. 32–36, Jan. 2008.
- [8] M. Fabbri, "Magnetic flux density and vector potential of linear polyhedral sources," *COMPEL-Int. J. Comput. Math. Elect. Electron. Eng.*, vol. 28, no. 6, pp. 1688–1700, 2009.
- [9] P. Bettini and R. Specogna, "A boundary integral method for computing eddy currents in thin conductors of arbitrary topology," *IEEE Trans. Magn.*, vol. 51, no. 3, Mar. 2015, Art. ID 7203904.
- [10] M. Bandinelli *et al.*, "A surface PEEC formulation for high-fidelity analysis of the current return networks in composite aircrafts," *IEEE Trans. Electromagn. Compat.*, vol. 57, no. 5, pp. 1027–1036, Oct. 2015.
- [11] G. Rubinacci and A. Tamburrino, "Automatic treatment of multiply connected regions in integral formulations," *IEEE Trans. Magn.*, vol. 46, no. 8, pp. 2791–2794, Aug. 2010.
- [12] T.-T. Nguyen, G. Meunier, J.-M. Guichon, and O. Chadebec, "3-D integral formulation using facet elements for thin conductive shells coupled with an external circuit," *IEEE Trans. Magn.*, vol. 51, no. 3, Mar. 2015, Art. ID 6300504.
- [13] V. Le-Van, G. Meunier, O. Chadebec, and J.-M. Guichon, "A volume integral formulation based on facet elements for nonlinear magnetostatic problems," *IEEE Trans. Magn.*, vol. 51, no. 7, Jul. 2015, Art. ID 7002206.
- [14] T.-S. Nguyen, J.-M. Guichon, O. Chadebec, G. Meunier, and B. Vincent, "An independent loops search algorithm for solving inductive PEEC large problems," *Prog. Electromagn. Res. M*, vol. 23, pp. 53–63, 2012.
- [15] R. Albanese and G. Rubinacci, "Integral formulation for 3D eddy-current computation using edge elements," *IEE Proc. A, Phys. Sci., Meas. Instrum., Manage. Edu.-Rev.*, vol. 135, no. 7, pp. 457–462, Sep. 1988.